Tidal variation and litter decomposition co-affect carbon emissions in estuarine wetlands

Yu Peng [a,1], Chuanqiao Zhou [a,1], Qiu Jin [b], Ming Ji [a], Feiyu Wang [a], Qian Lai [a], Ruijie Shi [a], Xiaoguang Xu [a,*], Liangang Chen [b], Guoxiang Wang [a]

[a] School of Environment, Nanjing Normal University, Jiangsu Center for Collaborative Innovation in Geographical Information Resource Development and Application, Jiangsu Key Laboratory of Environmental Change and Ecological Construction, Nanjing 210023, China
[b] State Key Laboratory of Hydrology-Water Resources and Hydraulic Engineering, Nanjing Hydraulic Engineering, Nanjing Hydraulic Research Institute, Nanjing 210029, China

HIGHLIGHTS

- Carbon emissions varied in different vegetation cover areas in estuarine wetlands.
- Different litter decomposition affected the competition of MPA and MOB in soils.
- The organic carbon content of litters affected the carbon emission capacity.
- Tidal variation contributed more to carbon emissions on the daily timescale.
- Litter decomposition contribution to carbon emissions increased with prolonged timescales.

GRAPHICAL ABSTRACT
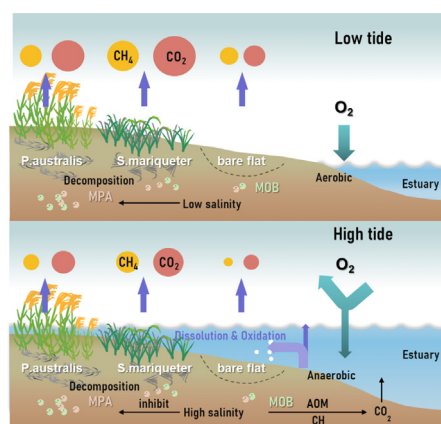
ABSTRACT

Estuarine wetlands play important roles in the regional and global carbon cycle as well as greenhouse gas emissions; however, the driving factors and potential carbon emissions mechanisms are unclear. Here, the carbon emission fluxes were investigated in situ from different vegetated areas in the Chongming wetlands. The results showed that the highest methane (CH_4) and carbon dioxide (CO_2) emissions of 178.1 and 21,482.5 $mg \cdot m^{-2} \cdot min^{-1}$ were in *Scirpus mariqueter* and *Phragmites australis* dominated areas, respectively. A series of microcosms was strategically designed to simulate the influence of tidal variation on carbon emissions and the litter decomposition on daily- and monthly-timescales in estuarine wetlands. All added litter promoted CH_4 and CO_2 emissions from the wetland soils. The CH_4 and CO_2 emission fluxes of the *S. mariqueter* treatment were higher (367.7 vs. 108.4; 1607.9 vs. 1324.3 $mg \cdot m^{-2} \cdot min^{-1}$) than those of the *P. australis* treatment without tidal variation on a monthly timescale, due to the higher total organic carbon (TOC) content of *S. mariqueter*. The decomposition of litter also released a large amount of nutrients, which enhanced the abundance of methane-producing archaea (MPA) and methane-oxidizing bacteria (MOB). However, the tidal water level was negatively correlated with CH_4 and CO_2 emission fluxes. The CH_4 and CO_2 emission fluxes in the *S. mariqueter* treatment at the lowest tide were 556.02 and 604.99 $mg \cdot m^{-2} \cdot min^{-1}$, respectively. However, the CH_4 and CO_2 emission fluxes did not change significantly on the daily timescale in the *S. mariqueter* treatment without

* Corresponding author at: 1, Wenyuan Road, Xianlin University District, Nanjing 210023, China.
  E-mail address: xxg05504118@163.com (X. Xu).
[1] Both authors contributed equally.

tidal variations. Therefore, the prolonged timescales revealed increases in litter decomposition but a decrease in the contribution of tidal variations to carbon emissions in estuarine wetlands. These findings provide a theoretical basis for evaluating the carbon cycle in estuarine wetlands.

1. Introduction

The increase in greenhouse gas (GHG) emissions due to human activities has become one of the most serious environmental problems worldwide (Poulter et al., 2017; Sepulveda-Jauregui et al., 2018). It has been reported that CO_2, CH_4, and N_2O concentrations have increased by 47.3%, 156%, and 23.0%, from 1750 to 2019, respectively (IPCC, 2021). Estuarine wetlands generally act as a carbon sink; however, recent studies have shown that they may play a crucial role as a GHG carbon source (Yang et al., 2017; Tan et al., 2020). Therefore, exploring GHG emissions and the driving factors is significant to evaluate the carbon cycle and policy management for carbon sequestration in estuarine wetlands.

Many studies have demonstrated that tidal variations in estuarine wetlands affect carbon cycling in a variety of ways (Chauhan et al., 2015; Chamberlain et al., 2016). Tidal variations include different tidal phases, and as a result, the soils in wetlands are periodically submerged by tides or exposed to the atmosphere, which has an important effect on carbon cycling (Enright et al., 2013). The changes in soil salinity caused by tidal variations affect microbial activities and abundance, and thus are particularly important for carbon emissions (Qu et al., 2018; Yang et al., 2019; Mueller et al., 2020). When the soil is highly saline (Neubauer, 2013), the CH_4 production pathway changes and the methylotrophic CH_4 production pathway accounts for 90% of CH_4 emissions (Min and Zinder, 1989; Parkes et al., 2007). In contrast, anaerobic oxidation of methane (AOM), involving the oxidation processes of chemically inactive CH_4 to CO_2 catalyzed by microorganisms, oxidizes a large amount of CH_4 and increases CO_2 emissions and net total carbon output in estuarine wetlands due to high SO_4^{2-} concentrations (Olefeldt et al., 2017; Zhou et al., 2022). The changes in the soil redox environment induced by tidal variations also affect the abundance and activities of microbes as well as carbon emissions. The anaerobic environment in the soil promotes organic carbon mineralization at high tide (Luo et al., 2019), while the oxygen content in the soil increases at ebb tide, leading to CH_4 aerobic oxidation and a decrease in organic carbon mineralization (Yu et al., 2006). Therefore, the ebb and flow of tides change the microenvironment, the physicochemical properties, the microbial communities, and the function of the soil; thus, their effects on the carbon cycle in estuarine wetlands are dynamic and complex.

Different types of plants are generally distributed in strips depending on the height of the tidal variations in an estuarine wetland (Swarth et al., 2013; Wang et al., 2014). The growth and decomposition of these plants affect the carbon cycle in estuarine wetlands (McClain et al., 2003; Vidon et al., 2010). For example, *P. australis* and *S. mariqueter* are the main vegetation in estuarine wetlands (Zhang et al., 2017). *P. australis* is primarily located in the mid-high tide strip and has a longer period of development than *S. mariqueter*, which is located in the lower tide strip with a short development time (Li et al., 2017). Different types of plants affect the distribution of organic carbon stocks (Lehmann and Kleber, 2015; Li et al., 2017). It has been reported that 10–40% of plant photosynthates enter the soil through root exudation, while the rest enter the soil as litter (Lu and Conrad, 2005). The physiological characteristics of different plant species produce different qualities and quantities of root exudations. Owing to substrate selection and affinity, these root exudations directly affect the substrate supply of microorganisms and change the microbial activities and community structure with subsequent carbon emissions in estuarine wetlands (Lu and Conrad, 2005; Koelbener et al., 2010; Inglett et al., 2012; Yuan et al., 2014). In contrast, the carbon content of the litter generated by different plant species is different and is affected by many factors during decomposition (Duan et al., 2018). Rapidly alternating dry and wet conditions lead to significant changes in dissolved oxygen, which is conducive to litter decomposition (Shi et al., 2015). The decomposition rate may

gradually decrease as the litter decomposes from leaching during the early decomposition stage and from microbial decomposition during the late decomposition stage (Bray et al., 2012; Hossain et al., 2014). However, the litter decomposition and carbon emission processes in estuarine wetlands are on a relatively long timescale. Under the influence of the daily cycle of tidal variations, the driving mechanisms of these biogeochemical processes may change and require further investigation.

In this study, we collected gas samples from different vegetated areas in the Chongming wetlands to test the carbon emission characteristics under the influence of litter species and tidal variations. In addition, a series of microcosmic systems were systemically constructed to explore the effects of tidal variation and litter decomposition on carbon output, particularly GHG emissions, from estuarine wetlands. The variations in the nutrients in the overlying water, the abundance of soil microbes, and GHG emissions were intensively investigated on daily and monthly timescales. The findings from this study will provide a theoretical basis for evaluating the carbon output capacity of estuarine wetlands.

2. Materials and methods

2.1. Study site and sample collection

Samples of soils, *P. australis* and *S. mariqueter* plants, and the overlying water were collected from the Chongming wetlands (31°79′41″ N, 121°47′40″ E) in July 2020. The plant samples were washed and killed at 105 °C for 30 min. The soil samples were homogenized thoroughly and placed in polyethylene bags. The overlying water was filtered through a 250-mesh plankton mesh and stored in an incubator with ice packs. Gas samples were collected via static chambers every 10 min for 1 h with three replicates (Zhou et al., 2021). All samples were immediately transported to the laboratory for further analysis.

2.2. Set-up of the microcosm systems

The microcosm systems for simulating the tidal variations and decomposition of the different litter species consisted of 18 acrylic tubes (diameter 80 mm and height 700 mm) and each treatment had three replicates (Fig. S1). A 400 g portion of homogenized soil was added to each tube (about 5 cm depth), and then 5 g of *P. australis* or *S. mariqueter* litter, cut into about 1 × 1 mm pieces, was added to the systems. The control was simultaneously set without plants.

The water level changes were adjusted according to the tidal variations of the Chongming wetlands during autumn (Liu et al., 2015). The control system of water circulation was composed of two peristaltic pumps, four silicone tubes and a small water storage tank. The simulated tidal variations completed two cycles over 24 h, with the highest water level reaching 25 cm at 0:00 am and 12:00 pm (Fig. S2).

All of the microcosm systems were stabilized for about 2 weeks at 25 °C. All of the systems were sampled on 1, 4, 7, 10, 13, 16, 21, 24, and 27 d. Water and gas were collected using the continuous sampling method. The gas samples were collected via a syringe from the headspace of the microcosm every 10 min for 1 h. All water columns were filtered through 0.45 μm nylon filters. The initial and final sediment samples were collected and stored at −80 °C for further analysis.

2.3. Chemical analysis

2.3.1. Determination of TN, TP, and TOC concentrations

The overlying water samples were used to determine the concentrations of total phosphorus (TP), total nitrogen (TN) and total organic carbon

(TOC). TP and TN were measured using ammonium molybdate spectrophotometric method and an ultraviolet spectrophotometry method through UV–Visible spectrophotometer (UV-6100, Mapada, China). TOC was investigated using a TOC analyzer (AnlaytikJena HT1300, Germany). TP, TN and TOC concentrations were measured with an accuracy of up to 0.1 mg/L level.

2.3.2. CH₄ and CO₂ emission fluxes

The CH_4 and CO_2 emission fluxes (*F*) were estimated by the static chamber method using the following equation:

$$F = \frac{M}{V_0} \frac{P}{P_0} \frac{T_0}{T} H \frac{dc}{dt}$$

where *F* is the CH_4 and CO_2 emissions fluxes ($\mu g \cdot m^{-2} \cdot min^{-1}$); *M* is the molar mass of the CH_4 and CO_2 being measured (g·mol); *P* is the pressure at sampling (Pa), *T* is the temperature at sampling (K); V_0, P_0 and T_0 are the molar volume of the CH_4 and CO_2, the absolute air pressure and the temperature of the air under the standard state; *H* is the height above the water surface of the static box (m); *dc/dt* is the slope of gas concentration changing with time during sampling; it is obtained by linear regression of gas concentration at different time and corresponding time interval.

2.3.3. Measurement of CH₄ and CO₂ concentrations

CH_4 and CO_2 samples were measured using a gas chromatograph (Shimadzu, GC-2014C). 10 mL of gas were withdrawn from the microsystems. The chamber temperature and FID detector temperatures were 55 °C and 200 °C, respectively. The rate of the carrier gas was 2 mL/min by 99.999% high purity nitrogen. High purity hydrogen and air were used as the gas at a flow rate of 40 mL/min and 400 mL/min respectively. The detection limit was 0.2 ppm for CH_4 and 4 ppm for CO_2 with an error range of ± 1%.

2.4. Quantification of MPA and MOB in soils

The microbial communities and cell copy numbers of MPA and Methane oxidation bacteria (MOB) in soil were determined at day 0 (the initial stage) and 27 (the final stage) through sequencing and real-time reverse transcriptase quantitative polymerase chain reaction (RT-qPCR) techniques. The soil samples were collected and frozen at −80 °C in an ultra-low temperature freezer. The E.Z.N.A. ®Soil DNA Kit (Omega Bio-Tek, Norcross, GA, USA) was used to extract the total genomic DNA from each soil sample per the manufacturer's instructions. Nucleic acid mass and concentration were determined by 1% agarose gel electrophoresis and NanoDrop 2000 UV spectrophotometer (Thermo Scientific, USA), respectively. The MPA and MOB genes (*dmpA* and *pmoA*), were amplified using promers 1106F/1378r and A189F/mb661R, respectively. The ChamQ SYBR Color qPCR Master Mix

was be used as the signal dye q-PCR and the experiments were performed on an ABI7300 qPCR instrument (Applied Bi osystems, USA). Each 20 μL reaction mixture contained 2 μL of template DNA and 16.5 μL of ChamQ SYBR Color qPCR Master Mix. Standard curves for each gene were acquired by tenfold serial dilutions of standard plasmids that included the target functional gene. All procedures were performed following the MIQE guidelines.

2.5. Statistical analysis

Bivariate correlation analysis was used for correlation analysis. One-way analysis of variance (ANOVA) was used to analyse significant differences in microbial abundance over time and independent sample *t*-tests were used to determine the significance of the effects of letter species and tidal changes. All of the statistical analysis were conducted using the Statistical Package for the Social Sciences 18.0 (SPSS 18.0).

3. Results

3.1. CO₂ and CH₄ emission fluxes in the field

Significant differences were observed for CO_2 and CH_4 emission fluxes in the *P. australis* and *S. mariqueter* bare flats of the Chongming wetlands (Fig. 1). The CO_2 and CH_4 emission fluxes in the bare flats were lower than those in other areas, with values of 2226.7 and 25.5 $mg \cdot m^{-2} \cdot min^{-1}$, respectively. The CO_2 emission fluxes in the *P. australis* dominant area were the highest at 21,482.5 $mg \cdot m^{-2} \cdot min^{-1}$, which was 2.3 times the CO_2 emission flux in the *S. mariqueter* dominant area. The highest CH_4 emission flux was 178.1 $mg \cdot m^{-2} \cdot min^{-1}$ in the *S. mariqueter* dominant area, which was 1.7 times the CH_4 emission flux in the *P. australis* dominant area.

3.2. Dynamics of TOC, TN, and TP concentrations in the microcosms

The TOC, TN, and TP concentrations during litter decomposition increased in the overlying water and then decreased to a stable concentration (Fig. 2). The tidal variations did not affect the changes in the TOC, TN, or TP concentrations. The TOC, TN, and TP concentrations were the lowest in the bare flat treatments, except for the TN concentration in the tidal variation treatment. The TOC concentrations in the *S. mariqueter* treatments were higher than those in the *P. australis* treatments, and the highest concentrations with and without tidal variations were 77.6 and 89.7 mg/L, respectively. However, the TN and TP concentrations in the *P. australis* treatment were higher than in the *S. mariqueter* treatment. The TN concentrations in the *P. australis* treatment increased initially and then decreased quickly, with the lowest concentrations of 1.9 and 1.6 mg/L with and without tidal variations, respectively. The TP concentrations in the overlying water increased and then decreased to a stable concentration, with final
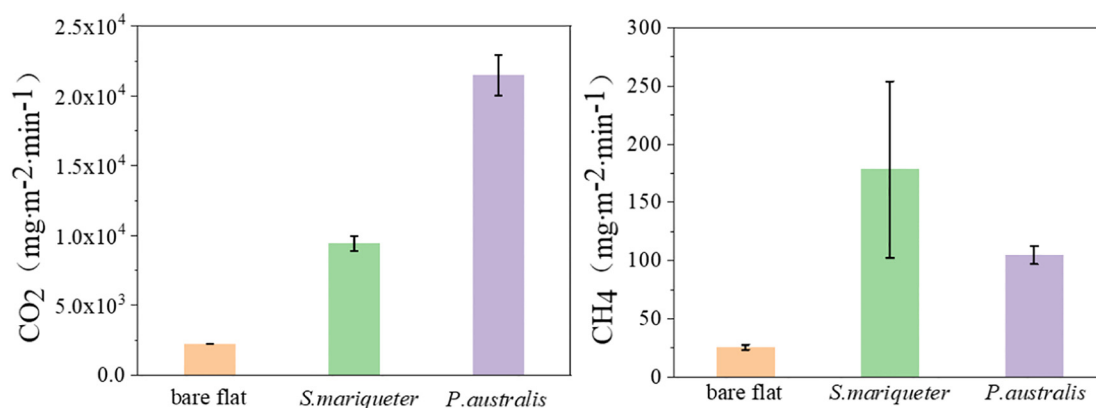

Fig. 1. CO_2 (left) and CH_4 (right) emission fluxes in different locations of Chongming wetland.
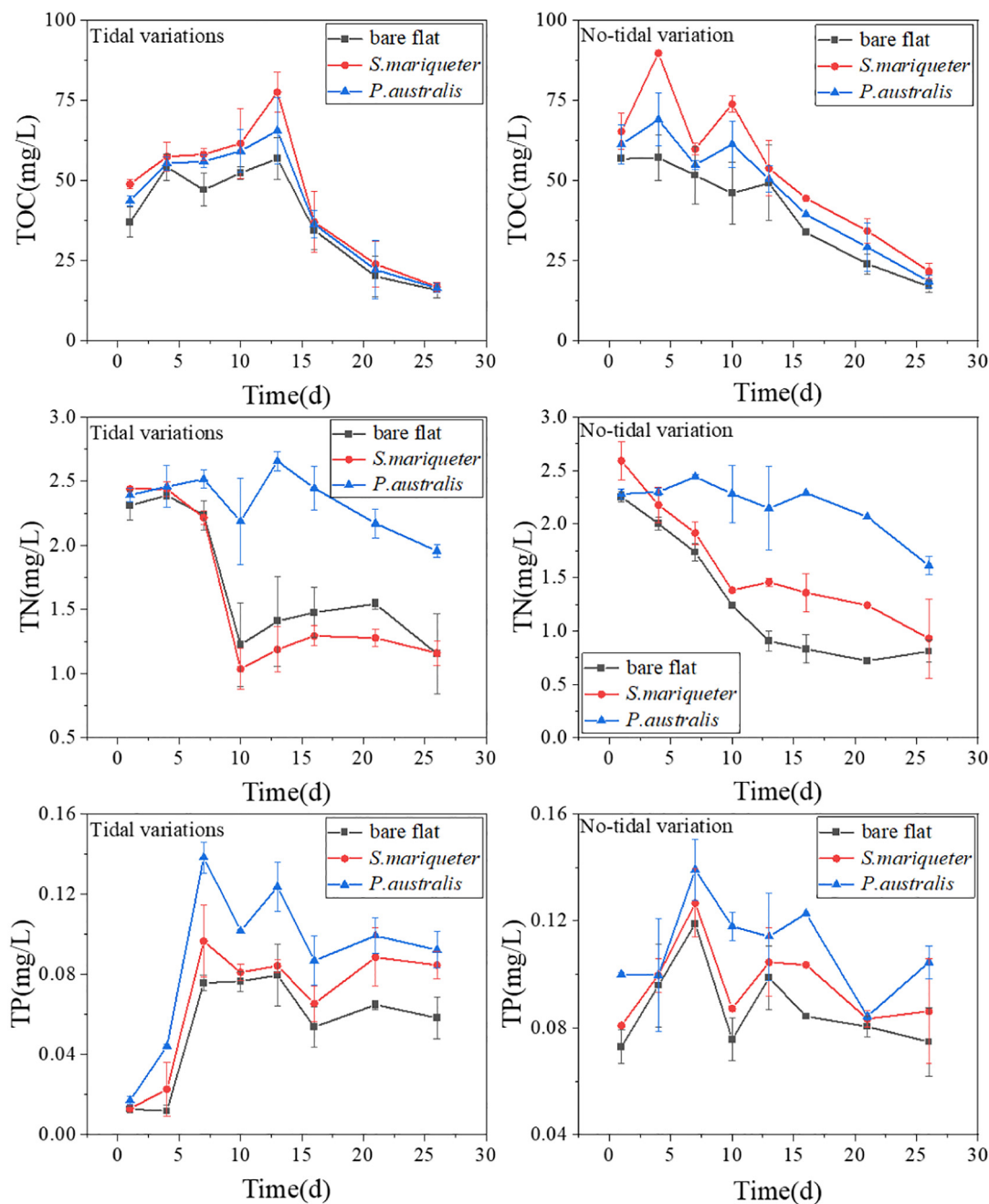
Fig. 2. Dynamic change of TOC, TN and TP dynamics in the overlying water with the tidal variations (left) and No-tidal variation (right).

TP concentrations of 0.09 and 0.1 mg/L in the *P. australis* treatment with and without tidal variations, respectively.

3.3. CO_2 and CH_4 emission fluxes on a monthly timescale in the microcosms

The long-term CO_2 and CH_4 emission fluxes increased initially and then decreased significantly during incubation (Fig. 3). The lowest CO_2 and CH_4 emission fluxes were in the bare flat treatment. The CO_2 and CH_4 emission fluxes in the *S. mariqueter* treatment were higher than those in the *P. australis* treatment with and without tidal variations. The highest CO_2 emission flux was 2701.8 $mg·m^{-2}·min^{-1}$, which occurred in the *S. mariqueter* treatment with tidal variations on day 10. The highest CO_2 emission flux was 1607.9 $mg·m^{-2}·min^{-1}$ on day 7 in the *S. mariqueter* treatment without tidal variations. The final CO_2 emission fluxes were 564.3 and 164.6 $mg·m^{-2}·min^{-1}$ in the *P. australis* treatments with and without tidal variations, respectively. The highest CH_4 emission flux was 367.6

$mg·m^{-2}·min^{-1}$ on day 10 in the *S. mariqueter* treatment without tidal variations. The highest CH_4 emission flux was 310.7 $mg·m^{-2}·min^{-1}$ on day 13 in the *S. mariqueter* treatment with tidal variations. The highest CH_4 emission flux was 108.4 $mg·m^{-2}·min^{-1}$ on day 7 in the *P. australis* treatment without tidal variations, and the highest CH_4 emission flux was 106.1 $mg·m^{-2}·min^{-1}$ on day 16 in the *P. australis* treatment with tidal variations.

3.4. Dynamics of soil MPA and MOB

The abundances of MPA and MOB increased in the *P. australis* and *S. mariqueter* treatments, while they decreased significantly in the bare flat treatments (Fig. 4). The initial abundances of MPA and MOB in the *P. australis* treatments were higher than the other treatments at 3.5×10^6 and 7.6×10^6 copies/g, respectively. The abundances of MPA and MOB in the treatments without tidal variations were higher than those with tidal variations. The highest abundance of MPA was 1.3×10^7 copies/g
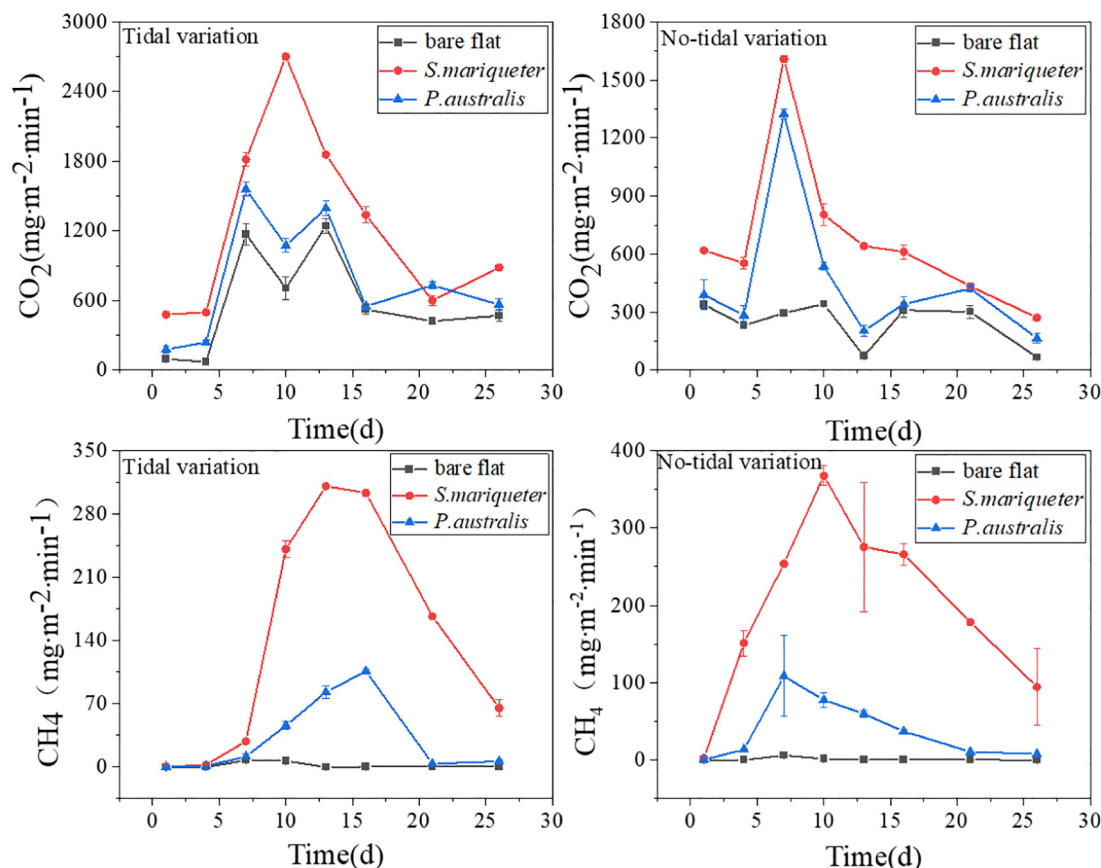
Fig. 3. Long-term CO_2 (left) and CH_4 (right) emission fluxes in different microcosms with the tidal variation (left) and no-tidal variation (right).

in the *S. mariqueter* treatment without tidal variations. The abundance of MOB was 1.3×10^7 copies/g in the *P. australis* treatment without tidal variations, which was higher than in the other treatments.

3.5. CO_2 and CH_4 emission fluxes on a daily timescale in the microcosms

The CO_2 and CH_4 emission fluxes changed with the tide. CO_2 and CH_4 emission fluxes decreased during the daily increase in the water level in the microcosms. The CO_2 and CH_4 emission fluxes did not change significantly in the treatments without tidal variations. The CO_2 and CH_4 emission fluxes were 2172.8 and 556.1 $mg \cdot m^{-2} \cdot min^{-1}$, respectively when the water level was the lowest during the second tidal variation in the *S. mariqueter* treatment. The CO_2 and CH_4 emission fluxes in the bare flats with tidal variations were lowest daily. CO_2 and CH_4 remained relatively stable in the

treatments with no tidal variation. The highest CO_2 and CH_4 emission fluxes were in the *S. mariqueter* treatments, compared to the values in the bare flats. The final CO_2 and CH_4 concentrations in the *S. mariqueter* treatments were 190.1 and 27.7 $mg \cdot m^{-2} \cdot min^{-1}$, respectively.

4. Discussion

CH_4 and CO_2 are the main forms of carbon emissions in estuarine wetlands (Yang et al., 2017; Amaral et al., 2021). Many factors affect CH_4 and CO_2 emissions in estuarine wetlands, such as the vegetation types, the tides, and temperature (Hu et al., 2017; Jacotot et al., 2018). It has been reported that wetlands have a large carbon sink function under long-term flooding because long-term flooding weakens microbial activities and slows litter decomposition (Keller et al., 2013). In addition, the
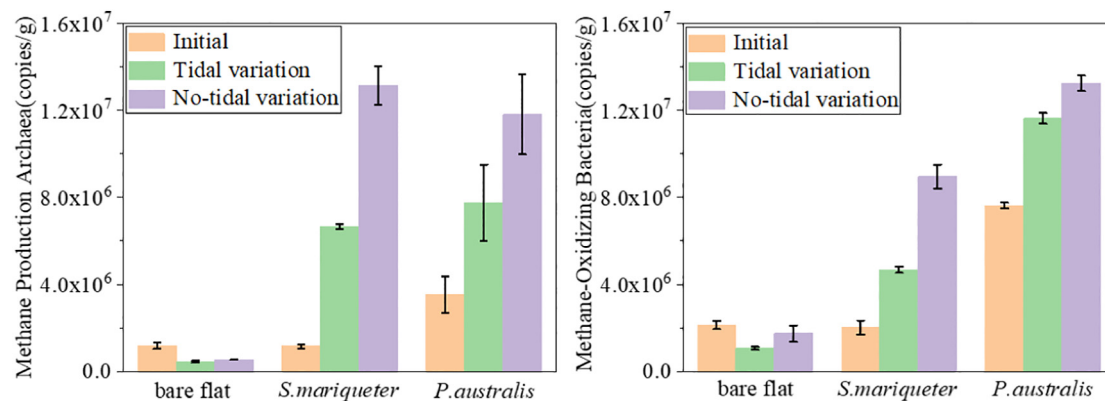

Fig. 4. Dynamic changes of MPA and MOB in soils of different microcosms.

carbon emissions capacity of different areas (CH_4 and CO_2) in the Chongming wetlands were different (Fig. 1). The vegetation type is one of the main reasons for the significant difference in carbon emission fluxes in wetlands, including production and emission processes (Askaer et al., 2011; Sun et al., 2012; Hsieh et al., 2021). Due to long-term flooding, the aerenchyma of wetland vegetation has evolved to adapt to the anaerobic environment (Yan et al., 2010). CH_4 and CO_2 enter the plant through free transport and travel from the rhizosphere to the atmosphere, which greatly promotes CH_4 and CO_2 emissions (Koelbener et al., 2010; Rice et al., 2010). When the litter falls into the wetland soil, the decomposition of the litter releases a large amount of organic carbon and enhances the carbon sink function of the wetland soil (Pancotto et al., 2010; Yarwood, 2018). The root exudates are also the important sources of soil organic carbon during plant growth which promotes the organic carbon mineralization (Zhou et al., 2018). Therefore, tidal variations and the species of litter are the main factors driving the difference in carbon emissions capacity of wetlands.

Litter is one of the main sources of soil organic carbon in wetlands (Pancotto et al., 2010), and the quantity and quality of the litter vary greatly among different plants, which changes the formation mechanism and accumulation rate of soil organic carbon (Hughes et al., 2006; Zhou et al., 2018). This is also an important factor affecting CH_4 and CO_2 emissions. In this study, the organic carbon content of *S. mariqueter* was higher than that of *P. australis* (Fig.S3). Litter with a high organic carbon content probably provides more substrate for utilization by microbes during decomposition (Wang et al., 2016; Ma et al., 2020). The abundance and activities of microorganisms, e.g., MPA and MOB (Fig. 4) affected CH_4 emissions. The CH_4 emissions from wetlands into the atmosphere are the final result of the combined action of MPA and MOB (Roland et al., 2017). In this study, the abundance of MPA in the *S. mariqueter* treatment was higher than that in the *P. australis* treatment (Fig. 4), and the abundance of MOB in the *P. australis* treatment was higher than that in the *S. mariqueter* treatment because different amounts of organic carbon were released during the

decomposition of different litters (Pancotto et al., 2010; Yakimovich et al., 2018). In addition, the released phosphorus and nitrogen to the water also provided the important substrates for the growth of microorganism during litter decomposition (Fig. 2). A study of peatlands in Alaska, USA showed that MPA abundance and structure, as well as terminal decomposition pathways, were closely related to the vegetation type (Hines et al., 2008). Therefore, the CH_4 emissions in the *S. mariqueter* treatments were higher than those in the *P. australis* treatments (Fig. 3). Different vegetation types produce different qualities and quantities of organic carbon, thus affecting the rate of CH_4 production. Therefore, the higher organic carbon content of *P. australis* during litter decomposition changed microbial abundance and the community structure and released more carbon; one part was released to the overlying water to increase the carbon and nutrient concentrations, and the other part was released to the atmosphere in the form of CH_4 and CO_2 (Fig. 3).

Tidal variation is another important factor that affects carbon emissions in estuarine wetlands (Knowles, 2002; Wei et al., 2020). In this study, CH_4 and CO_2 emissions were significantly affected by tidal variations on the daily timescale (Figs. 5; 6). When the tide was high, the emission fluxes of CH_4 and CO_2 were low ($R^2 = 0.8$ and 0.78). A high tidal level prevented the release of CH_4 and CO_2, as part of the CH_4 and CO_2 is dissolved or transported in the overlying water (Neubauer, 2013; Sanchez-Rodriguez et al., 2021). In addition, the high salinity of the soil in estuarine wetlands during the high tidal level inhibits microbial activities, including MPA and MOB (Poffenbarger et al., 2011; Neubauer, 2013), and the increased SO_4^{2-} concentration also inhibits CH_4 production through the competition of organic carbon source and AOM (Weston et al., 2006; Poffenbarger et al., 2011). Although the ebb and flow of the tides significantly affected carbon emissions on a daily timescale, it did not affect the monthly timescale because the vegetation type may be the main factor affecting carbon emissions of estuarine wetlands over a longer time scale (Figs. 3; 5) (Wei et al., 2020). From the short-term, particularly on the daily timescale, tidal variations lead to changes in the physical and chemical environment
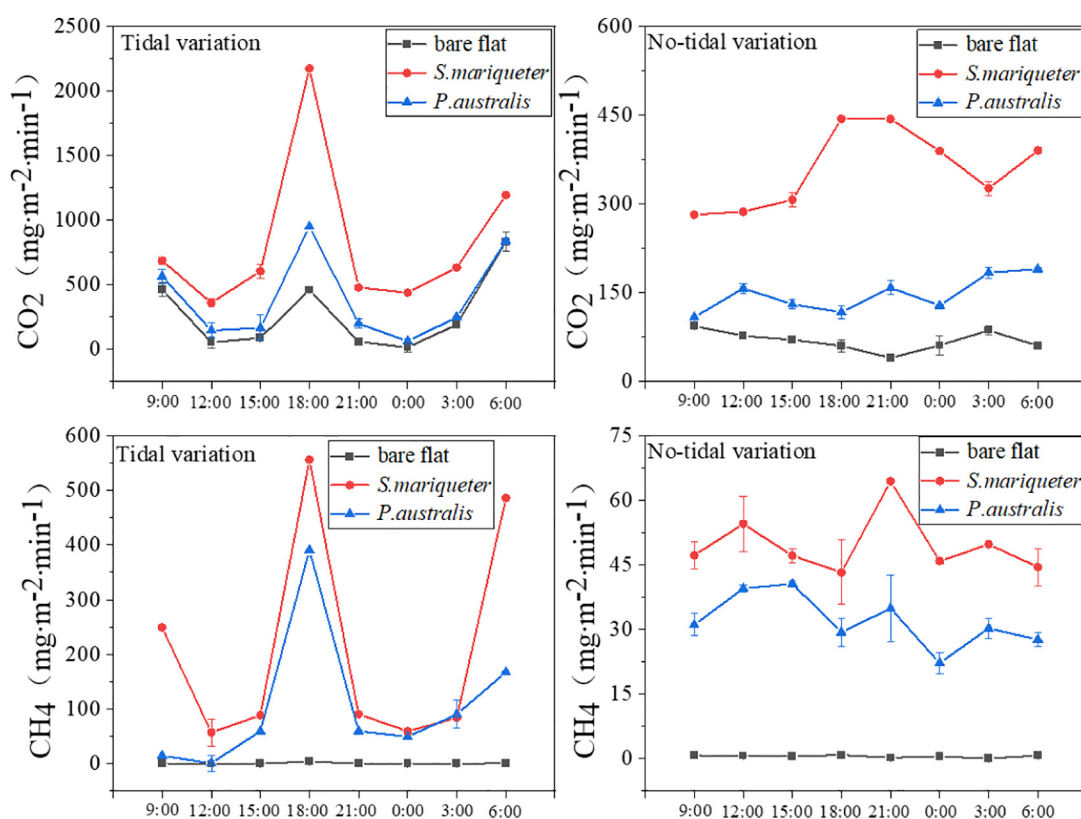

Fig. 5. CO_2 (left) and CH_4 (right) emission fluxes in different microcosms with the tidal variation (left) and no-tidal variation (right) in the daily timescale.
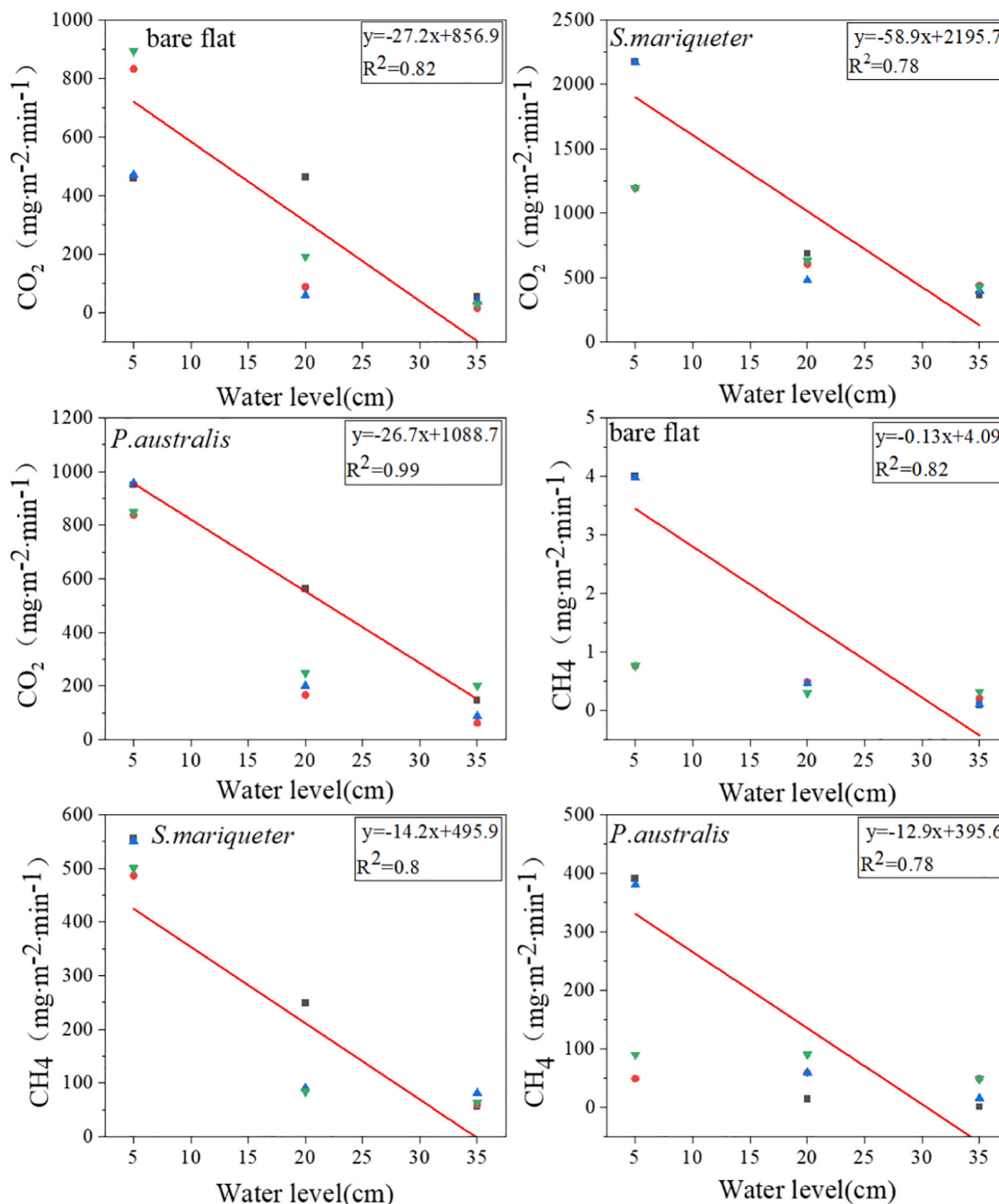
Fig. 6. Correlations between water levels and CO_2 and CH_4 emissions in different microcosms with the tidal variations.

which affected carbon emissions (Bakdwin et al., 2006; Preheim et al., 2016). However, litter decomposition is a long-term process, it did not affect carbon emissions due to the slow rate of decomposition during the initial stage (Figs. 3; 5). On the monthly timescale, the litter decomposition contribution to carbon emissions increased with the decomposition rate during the later stage, and the effect of tidal variations on carbon emissions gradually decreased (Figs. 3; 5). In addition, the rapid alternating dry-wet conditions caused by the tidal variations created aerobic and anaerobic conditions that enhanced refractory litter decomposition during the later stage. Therefore, an increase in the litter decomposition contribution occurs with a decrease in the tidal variation contribution to carbon emissions during prolonged timescales in estuarine wetlands.

A conceptual diagram was constructed to clarify the effects of tidal variations and litter decomposition on carbon emissions in estuarine wetlands (Fig. 7). The different qualities and quantities of litter enter the soil and produce spatio-temporal heterogeneity in the soil organic matter distribution in the estuarine wetlands. The organic carbon source is an important substrate for microbial growth; therefore, the abundance and activities of microorganisms, such as MPA and MOB, vary under the influence of different litter types. Tidal variation is another factor affecting CH_4 and CO_2 emissions. The anaerobic environments formed in the soil during high tide promote CH_4 and CO_2 production. Subsequently, saturated CH_4 and CO_2 are released from the soil into the atmosphere under the low tide. In addition, the effects of tidal variations on carbon emissions in estuarine wetlands varied at different timescales. Tidal variations had a significant effect on carbon emissions on the daily timescale; however, vegetation type gradually became the main factor influencing carbon emissions on the monthly timescale. Therefore, the long-term carbon emissions need to be considered when assessing the carbon emissions capacity of estuarine wetlands.
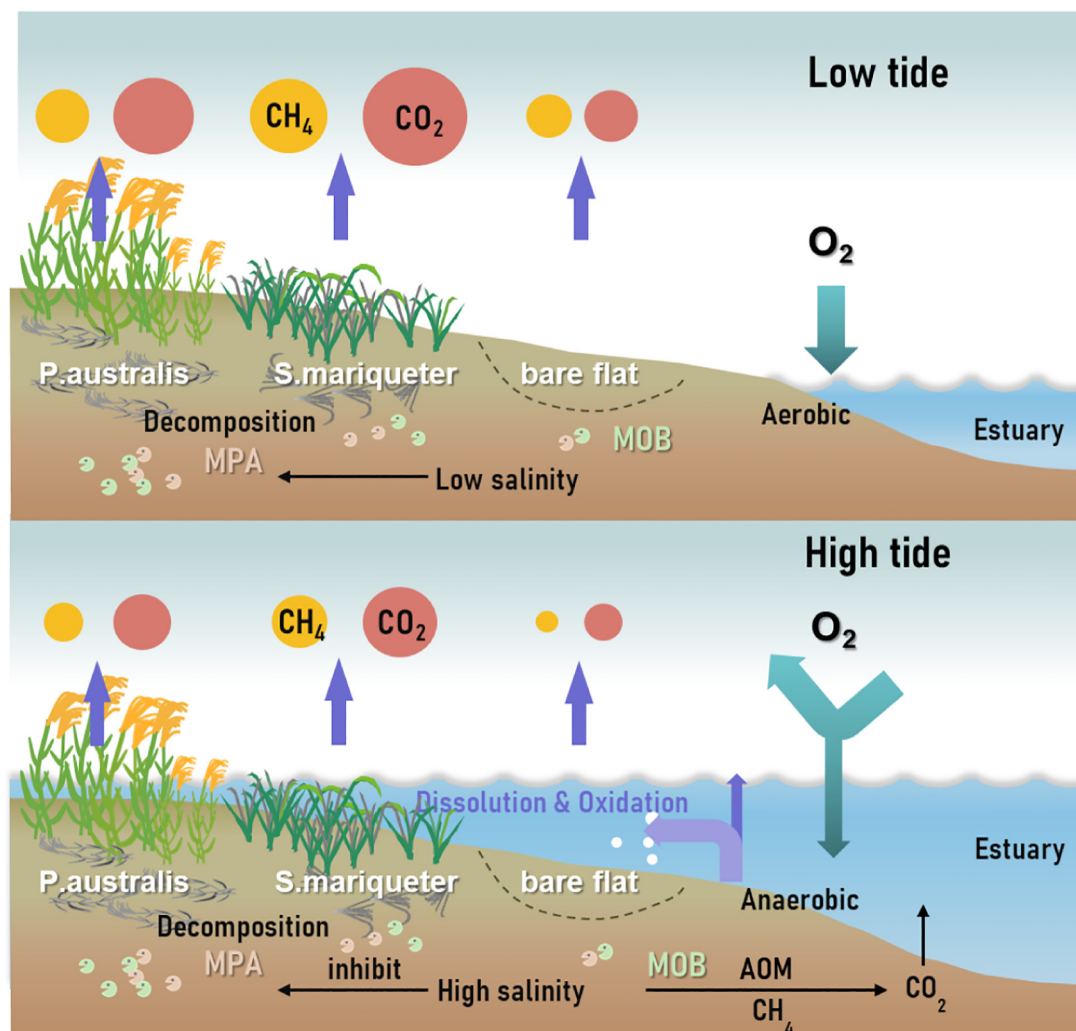
Fig. 7. A conceptual diagram of effects of tidal variation and litter decomposition on carbon cycling in estuarine wetlands.

5. Conclusion

Tidal variations and the litter species co-affected the carbon cycle of estuarine wetlands. An in situ investigation showed that the carbon content of different litter types was different. The higher the TOC content of the litter, the stronger the carbon emissions capacity. Litter decomposition promoted the growth of microorganisms, including MPA and MOB; thus, promoting carbon emissions from the estuarine wetlands. Tidal variations were also an important factor affecting carbon emissions in estuarine wetlands. The high-water level formed an anaerobic reduction environment to produce CH_4 and CO_2, however, they were oxidized in the water column and reduced the emission fluxes. Tidal variations significantly affected the carbon emissions on the daily timescale, while vegetation type was the main factor affecting carbon emissions of estuarine wetlands on the monthly timescale. Carbon emissions have a high sensitivity of tidal variations and vegetation types, with important implication for modeling greenhouse gas dynamics in estuarine wetlands.

Supplementary data to this article can be found online at https://doi.org/10.1016/j.scitotenv.2022.156357.

CRediT authorship contribution statement

Xiaoguang Xu, Liangang Chen, and Qiu Jin: designed and led the study. Yu Peng, Chuanqiao Zhou, Ming Ji, Feiyu Wang, Qian Lai, and Ruijie Shi: performed the investigation and analysed the samples. Yu Peng, Chuanqiao Zhou: wrote the original draft with major edits and inputs from Xiaoguang Xu, Qiu Jin and Guoxiang Wang.

Declaration of competing interest

The authors declare that they have no known competing financial interests or personal relationships that could have appeared to influence the work reported in this paper.

Acknowledgements

References

Amaral, V., Ortega, T., Romera-Castillo, C., Forja, J., 2021. Linkages between greenhouse gas (CO2, CH4, and N2O) and dissolved organic matter composition in a shallow estuary. Sci. Total Environ. 788, 147863.

Askaer, L., Elberling, B., Friborg, T., Jorgensen, C.J., Hansen, B.U., 2011. Plant-mediated CH4 transport and C gas dynamics quantified in-situ in a Phalaris aeundinacea-dominant wetland. Plant Soil 343 (1–2), 287–301.

Bakdwin, D.S., Rees, G.N., Mitchell, A.M., Watson, G., Williams, J., 2006. The short-term effects of salinization on anaerobic nutrient cycling and microbial community structure in sediment from a freshwater wetland. Wetlands 26 (2), 455–464.

Bray, S.R., Kitajima, K., Mack, M.C., 2012. Temporal dynamics of microbial communities on decomposing leaf litter of 10 plant species in relation to decomposition rate. Soil Biol. Biochem. 49, 30–37.

Chamberlain, S.D., Gomez-Casanovas, N., Walter, M.T., Boughton, E.H., Bernacchi, C.J., DeLucia, E.H., Groffman, P.M., Keel, E.W., Sparks, J.P., 2016. Influence of transient flooding on methane fluxes from subtropical pastures. J. Geophys. Res. Biogeosci. 121 (3), 965–977.

Chauhan, R., Datta, A., Ramanathan, A., Adhya, T.K., 2015. Factors influencing spatio-temporal variation of methane and nitrous oxide emission from a tropical mangrove of eastern coast of India. Atmos. Environ. 107, 95–106.

Duan, H., Wang, L., Zhang, Y.N., Fu, K.H., Tsang, Y.F., Wu, J.H., Le, Y.Q., 2018. Variable decomposition of two plant litters and their effevts on the carbon sequestration ability of wetland soil in the Yangtze River estuary. Geoderma 319, 230–238.

Enright, C., Culberson, S.D., Burau, J.R., 2013. Broad timescale forcing and geomorphic mediation of tidal marsh flow and temperature dynamics. Estuar. Coasts 36 (6), 1319–1339.

Hines, M.E., Duddleston, K.N., Rooney-Varga, J.N., Fields, D., Chanton, J.P., 2008. Uncoupling of acetate degradation from methane formation in Alaskan wetlands: connections to vegetation distribution. Glob. Biogeochem. Cycles 22 (2), GB2017. https://doi.org/10.1029/2006GB002903.

Hossain, M., Siddique, M.R.H., Abdullah, A.M.R., Saha, S., Ghosh, D.C., Rahman, M.S., Limon, S.H., 2014. Nutrient dynamics associated with leaching and microbial decomposition of four abundant mangrove species leaf litter of the Sundarbans,Bangladesh. Wetlands 33 (3), 439–448.

Hsieh, S.H., Yuan, C.S., Ie, I.R., Yang, L., Lin, H.J., Hsueh, M.L., 2021. In-situ measurement of greenhouse gas emissions from a coastal estuarine wetland using a novel continuous monitoring technology: comparison of indigenous and exotic plant species. J. Environ. Manag. 281, 111905.

Hu, M.J., Ren, H.C., Ren, P., Li, J.B., Wilson, B.J., Tong, C., 2017. Response of gaseous carbon emissions to low-level salinity increase in tidal marsh ecosystem of the Min River estuary, southeastern China. J. Environ. Sci. 52, 210–222.

Hughes, R.F., Archer, S.R., Asner, G.P., Wessman, C.A., McMurtry, C., Nelson, J., Ansley, R.J., 2006. Changes in aboveground primary production and carbon and nitrogen pools accompanying woody plant encroachment in a temperate savanna. Glob. Chang. Biol. 12, 1733–1747.

Inglett, K.S., Txiglett, P.W., Reddy, K.R., Osborne, T.Z., 2012. Temperature sensitivity of greenhouse gas production in wetland soils of different vegetation. Biogeochemistry 108, 77–90.

IPCC, 2021. Chapter 2: changing state of the climate system. AR6 Climate Change 2021: The Physical Science Basis.

Jacotot, A., Marchand, C., Allenbach, M., 2018. Tidal variability of CO2, and CH4, emissions from the water column within a Rhizophora mangrove forest (New Caledonia). Sci. Total Environ. 631–632, 334–340.

Keller, J.K., Sutton-Grier, A.E., Bullock, A.L., Megonigal, J.P., 2013. Anaerobic metabolism in tidal freshwater wetlands: plant removal effects on iron reduction and methanogenesis. Estuar. Coasts 36 (3), 457–470.

Knowles, N., 2002. Natural and management influences on freshwater inflows and salinity in the San Francisco Estuary at monthly to interannual scales. Water Resour. Res. 38 (12), 1–11.

Koelbener, A., Strom, L., Edwards, P.J., Venterink, H.O., 2010. Plant species from mesotrophic wetlands cause relatively high methane emissions from peat soil. Plant Soil 2010 (326), 147–158.

Lehmann, J., Kleber, M., 2015. The contentious nature of soil organic matter. Nature 528 (7580), 60–68.

Li, Z.W., Liu, C., Dong, Y.T., Chang, X.F., 2017. Response of soil organic carbon and nitrogen stocks to soil erosion and land use types in the Loess hilly-gully region of China. Soil Tillage Res. 166, 1–9.

Liu, X.W., Xia, Y.Q., Li, H.L., Xu, J.J., 2015. Influence of surface runoff and tides on water level in the nearshore of south Chongming Island. Geotech.Investig.Surv. 12, 37–54.

Lu, Y., Conrad, R., 2005. In Situ Stable Isotope Probing of Methanogenic Archaea in the Rice Rhizosphere. Science 309, 1088–1090.

Luo, M., Zhu, W.F., Huang, J.F., Liu, Y.X., Duan, X., Wu, J., Tong, C., 2019. Anaerobic organic carbon mineralization in tidal wetlands along a low-level salinity gradient of s subtropical estuary: rates, pathways, and controls. Geoderma 337, 1245–1257.

Ma, L., Jiang, X.L., Liu, G.H., Yao, L.G., Liu, W.Z., Pan, Y.T., Zuo, Y.X., 2020. Environmental factors and microbial diversity and abundance jointly regulate soil nitrogen and carbon biogeochemical processes in Tibetan wetlands. Environ. Sci. Technol. 54 (6), 3267–3277.

McClain, M.E., Boyer, E.W., Dent, C.L., Gergel, S.E., Grimm, N.B., Groffman, P.M., Hart, S.C., Harvey, J.W., Johnston, C.A., Mayorga, E., McDowell, W.H., Pinay, G., 2003. Biogeochemical hot spots and hot moments at the Interface of terrestrial and aquatic ecosystems. Ecosystems 6, 301–312.

Min, H., Zinder, S.H., 1989. Kinetics of acetate utilization by two thermophilic acetotrophic methanogens: Methanosarcina sp.strain CALS-1 and Methanothrix sp.strain CALS-1. Appl. Environ. Microbiol. 55, 488–491.

Mueller, P., Mozdzer, T.J., Langley, J.A., 2020. Plant species determine tidal wetland methane response to sea level rise. Nat. Commun. 11, 5154.

Neubauer, S.C., 2013. Ecosystem responses of a tidal freshwater marsh experiencing saltwater intrusion and altered hydrology. Estuar. Coasts 36 (3), 491–507.

Olefeldt, D., Euskirchen, E.S., Harden, J., Kane, E., McGuire, A.D., Waldrop, M.P., Turetsky, M.R., 2017. A decade of boreal rich fen greenhouse gas fluxes in response to natural and experimental water table variability. Glob. Chang. Biol. 23 (6), 2428–2440.

Pancotto, V.A., van Bodegom, P.M., van Hal, J., van Logtestijn, R.S.P., Blokker, P., Toet, S., Aerts, R., 2010. N deposition and elevated CO2 on methane emissions: differential responses of indirect effects compared to direct effects through litter chemistry feedbacks. J.Geophys.Res.Biogeosci. 115, G02001.

Parkes, R.J., Cragg, B.A., Banning, N., Brock, F., Webster, G., Fry, J.C., Hornibrook, E., Pancost, R.D., Kelly, S., Knab, N., Jørgensen, B.B., Rinna, J., Weightman, A.J., 2007. Biogeochemistry and biodiversity of methane cycling in subsurface marine sediments (Skagerrak, Denmark). Environ. Microbiol. 9, 1146–1161.

Poffenbarger, H.J., Needelman, B.A., Megonigal, P.J., 2011. Salinity influence on methane emissions from tidal marshes. Wetlands 31, 831–842.

Poulter, B., Bousquet, P., Canadell, J.G., Ciais, P., Peregon, A., Saunois, M., Arora, V.K., Beerling, D.J., Brovkin, V., Jones, C.D., Joos, F., Gedney, N., Ito, A., Kleinen, T., Koven, C.D., McDonald, K., Melton, J.R., Peng, C.H., Peng, S.S., Prigent, C., Schroeder, R., Riley, W.J., Saito, M., Spahni, R., Tian, H.Q., Taylor, L., Viovy, N., Wilton, D., Wiltshire, A., Xu, X.Y., Zhang, B.W., Zhang, Z., Zhu, Q.A., 2017. Global wetland contribution to 2000–2012 atmospheric methane growth rate dynamics. Environ. Res. Lett. 12, 9.

Preheim, S.P., Olesen, S.W., Spencer, S.J., Materna, A., Varadharajan, C., Blackburn, M., Friedman, J., Rodriguez, J., Hemond, H., Alm, E.J., 2016. Surveys, simulation and single-cell assays relate function and phylogeny in a lake ecosystem. Nat. Microbiol. 1 (9), 16130.

Qu, W., Li, J., Han, G., Wu, H., Song, W., Zhang, X., 2018. Effect of salinity on the decomposition of soil organic carbon in a tidal wetland. J. Soils Sediments 19, 609–617.

Rice, A.L., Butenhoff, C.L., Shearer, M.J., Teama, D., Rosenstiel, T.N., Khalil, M.A.K., 2010. Emissions of anaerobically produced methane by trees. Geophys. Res. Lett. 37, 1–5.

Roland, F.A.E., Darchambeau, F., Morana, C., Bouillon, S., Borges, A.V., 2017. Emission and oxidation of methane in meromictic, eutrophic and temperate lake (Dendre, Belgium). Chemosphere 168, 756–764.

Sanchez-Rodriguez, J., Sierra, A., Jimenez-Lopez, D., Ortega, T., Gomez-Parra, A., Forja, J., 2021. Dynamic of CO2, CH4 and N2O in the Guadalquivir estuary. Sci. Total Environ. 805, 150193.

Sepulveda-Jauregui, A., Hoyos-Santillan, J., Martinez-Cruz, K., Anthony, K.M.W., Casper, P., Belmonte-Izquierdo, Y., Thalasso, F., 2018. Eutrophication exacerbates the impact of climate warming on lake methane emission. Sci. Total Environ. 636, 411–419.

Shi, A.D., Yan, N., Marschner, P., 2015. Cumulative respiration in two drying and rewetting cycles depends on the number and distribution of moist days. Geoderma 243, 168–174.

Sun, X., Song, C., Guo, Y., 2012. Effect of plants on methane emissions from a temperate marsh in different seasons. Atmos. Environ. 60, 277–282.

Swarth, C.W., Delgado, P., Whigham, D.F., 2013. Vegetation dynamics in a tidal freshwater wetland: a long-term study at differing scales. Estuar. Coasts 36 (3), 559–574.

Tan, L.S., Ge, Z.M., Zhou, X.H., Li, S.H., Li, X.Z., Tang, J.W., 2020. Conversion of coastal wetlands, riparian wetlands, and peatlands increases greenhouse gas emissions: a global meta-analysis. Glob. Chang. Biol. 26 (3), 1638–1653.

Vidon, P., Allan, C., Burns, D., Duval, T.P., Gurwick, N., Inamdar, S., Lowrance, R., Okay, J., Scott, D., Sebestyen, S., 2010. Hot spots and hot moments in ripar- ian zones: potential for improve water quality management. J. Am. Water Res. Assoc. 46 (2), 278–298.

Wang, S.H., Wang, H.Q., Fang, Y., Li, K., 2014. Ability of plant carbon fixation in the coastal wetland of Chongming Island. Chin.J.Ecol. 33 (4), 915–921.

Wang, J.J., Liu, C.Y., Gong, X.F., Liu, Y.M., Chen, C.L., 2016. Trimethylamine stimulated and dissolved organic matter inhibited methane production in sediment from the Poyang Lake,China. Environ. Technol. 37 (20), 2545–2554.

Wei, S.Y., Han, G.X., Jia, X., Song, W.M., Chu, X.J., He, W.J., Xia, J.Y., Wu, H.T., 2020. Tidal effects on ecosystem CO2 exchange at multiple timescales in a salt marsh in the Yellow River Delta. Estuar.Coast.Shelf Sci. 238, 106727.

Weston, N.B., Dixon, R.E., Joye, S.B., 2006. Ramifications of increased salinity in tidal freshwater sediments: geochemistry and microbial pathways of organic matter mineralization. J.Geophys.Res.Biogeosci. 111 (G1), G01009.

Yakimovich, K.M., Emilson, E.J.S., Carson, M.A., Tanentzap, A.J., Basiliko, N., Mykytczuk, N.C.S., 2018. Plant litter type dictates microbial communities responsible for greenhouse gas production in amended lake sediments. Front. Microbiol. 9, 2662.

Yan, Q.X., Hong, X.Y., Sheng, C.X., 2010. Comparative Study on the Aerenchyma of Four Dominant Wetland Plants in Dongting Lake. 28, pp. 400–405.

Yang, W., Yuan, C.S., Tong, C., Yang, P., Yang, L., Huang, B.Q., 2017. Diurnal variation of CO2, CH4, and N2O emission fluxes continuously monitored in-situ in three environmental habitats in a subtropical estuarine wetland. Mar. Pollut. Bull. 119 (1), 289–298.

Yang, P., Wang, M.H., Lai, D.Y.F., Chun, K.P., Huang, J.F., Wan, S.A., Bastviken, D., Tong, C., 2019. Methane dynamics in an estuarine brackish Cyperus malaccensis marsh: production and porewater concentration in soils, and net emissions to the atmosphere over five years. Geoderma 337, 132–142.

Yarwood, S.A., 2018. The role of wetland microorganisms in plant-litter decomposition and soil organic matter formation: a critical review. FEMS microbiologyEcology 94 (11), fiy175.

Yu, K.W., Faulkner, S.P., Patrick, W.H., 2006. Redox potential characterization and soil greenhouse gas concentration across a hydrological gradient in a Gulf coast forest. Chemosphere 62 (6), 905–914.

Yuan, J., Ding, W., Liu, D.Y., Xiang, J., Lin, Y.X., 2014. Methane production potential and methanogenic archaea community dynamics along the Spartina alterniflora invasion chronosequence in a coastal salt marsh. Appl. Microbiol. Biotechnol. 98, 1817–1829.

Zhang, T.Y., Chen, H.P., Cao, H.B., Ge, Z.M., Zhang, L.Q., 2017. Combined influence of sedimentation and vegetation on the soil carbon stocks of a coastal wetland in the Changjiang estuary. Chin. J. Oceanol. Limnol. 35, 833–843.

Zhou, L., Li, H., Shen, H., Xu, Y., Wang, Y., Xing, A., Zhu, Y., Zhou, S., Fang, J., 2018. Effects of shrub encroachment on vertical changes in soil organic carbon in Mongolian grasslands: using a multibiomarker approach. Plant Soil 431, 217–230.

Zhou, Y.W., Xu, X.G., Song, K., Yeerken, S.B., Deng, M., Li, L., Riya, S., Wang, Q.L., Terada, A., 2021. Nonlinear pattern and algal dual-impact in N2O emission with increasing trophic levels in shallow lakes. Water Res. 203, 117489.

Zhou, C.Q., Peng, Y., Deng, Y., Yu, M.T., Chen, L., Zhang, L.Q., Xu, X.G., Zhao, F.J., Yan, Y., Wang, G.X., 2022. Increasing Sulfate Concentration and Sedimentary Decaying Cyanobacteria Co-affect Organic Carbon Mineralization in Eutrophic Lake Sediment. 806(3), p. 151260.